Local-field effects in the electric field gradient of dilute transition-metal alloys

J. Singh
Department of Physics, Panjab Agricultural University, Ludhiana-141004, India

S. K. Rattan and S. Prakash
Department of Physics, Panjab University, Chandigarh-160014, India
(Received 2 May 1988; revised manuscript received 1 August 1988)

A formalism is developed for impurity screening in a transition-metal (TM) dilute alloy in the dielectric screening approach. The full dielectric tensor is inverted using two schemes: (1) the linear combination of atomic orbitals approximation, and (2) the mixed-band-structure scheme, where s electrons are represented in the free-electron approximation and the d electrons in a local representation. In both schemes the exact expressions are obtained for the excess impurity scattering potential $\Delta V(\mathbf{r})$ and the impurity-induced charge perturbation $\Delta n(\mathbf{r})$. In the mixed-band-structure scheme, $\Delta V(\mathbf{r})$ and $\Delta \mathbf{n}(\mathbf{r})$ are separable into isotropic and anisotropic contributions. The latter is the manifestation of local-field (LF) effects. The numerical results for $\Delta V(\mathbf{r})$ and $\Delta n(\mathbf{r})$ are obtained for vanadium (V) alloys with TM impurities using a noninteracting-model band structure. The results are consistent with the other theoretical results and experimental predictions. The LF effects in $\Delta V(\mathbf{r})$ and $\Delta n(\mathbf{r})$ are found to be significant. The electric field gradient (EFG) is calculated for V alloys including LF effects. The calculations of the EFG suggest that both valence and size effects are equally important in explaining the experimental results.

I. INTRODUCTION

The theoretical study of electronic structure of the transition-metal (TM) impurities in cubic TM's, usually called transitional cubic alloys, is of immense importance both from the fundamental and technological points of views.[1] It involves two different aspects: first is the precise description of the electronic structure of the host metal through the electronic band structure calculations and second is a self-consistent solution of the scattering problem which is determined by the Hamiltonian of the host metal and the impurity scattering potential. The basic physical quantities of interest are the impurity scattering potential $\Delta V(\mathbf{r})$ and the impurity-induced charge perturbation $\Delta n(\mathbf{r})$, which can be used to study the different electronic properties of these alloys.[2]

In a pure TM the conduction electrons possess both the s and d characters. The s electrons are free to move in the crystal and suffer resonant scattering from the quasilocalized d electrons.[3] It has been proved that the major part of screening is carried out by d electrons in TM's.[4,5] The introduction of substitutional TM impurities in TM's makes a system characteristically difficult to study theoretically. In these alloys the s- and d-conduction electrons of the host TM suffer resonant scattering from the d orbitals of the TM impurity ion, leading to the formation of the virtual bound states under favorable circumstances.[1,2]

Von Meerwall and Rowland[6] studied experimentally the nature of $\Delta n(\mathbf{r})$ and EFG in dilute V alloys with the TM impurities and observed very small wipeout numbers and large values of the electric field gradient (EFG) at first-nearest-neighbor (1NN) sites of the impurity. Here, the wipeout numbers represent the number of perturbed host ions per impurity. Pal *et al.*[7] studied $\Delta n(\mathbf{r})$ and the EFG in dilute V-based alloys, with bcc structure using the partial wave method (essentially an asymptotic limit) in conjunction with pseudopotential theory. However, it is found that the preasymptotic effects are equally important in these alloys.[2] To account for the preasymptotic effects the screening of the TM impurities in V metal in the dielectric screening approach is described by a scalar dielectric function $\epsilon_H(\mathbf{K})$ of the host metal.[8] It takes into account the effect of the d electrons and gives $\Delta n(\mathbf{r})$ valid at all distances from the impurity. The above-mentioned calculations yield isotropic $\Delta V(\mathbf{r})$ and $\Delta n(\mathbf{r})$ and thus the effect of anisotropy of d states which gives rise to local-field (LF) effects is ignored.[9,10]

It is found that the LF effects play a significant role in explaining the electronic properties of TM's.[4,5] If one accounts for anisotropy of d electrons, the dielectric function in a TM becomes a tensor $\epsilon_H(\mathbf{K},\mathbf{K}')$, the off-diagonal elements of which are manifestations of the LF effects.[4,5] The use of $\epsilon_H(\mathbf{K},\mathbf{K}')$, in the impurity screening problem yields anisotropic $\Delta V(\mathbf{r})$ and $\Delta n(\mathbf{r})$ which are distinct along different symmetry directions.[11,12] These $\Delta n(\mathbf{r})$ are used to estimate EFG's. Therefore it is worthwhile to investigate the effect of LF's on the impurity screening and the EFG. The scheme of the paper is as follows. In Sec. II we describe the formalism for the impurity scattering in the dielectric screening approach and in Sec. III we apply it to calculate $\Delta V(\mathbf{r})$, $\Delta n(\mathbf{r})$, and the EFG for V alloys with TM impurities. The results are concluded in Sec. IV.

II. THEORY

The screened impurity potential $\Delta V(\mathbf{r})$ is related to its Fourier transform $\Delta V(\mathbf{K})$ by the relation

$$\Delta V(\mathbf{r})=\frac{1}{(2\pi)^3}\int \Delta V(\mathbf{K})e^{i\mathbf{K}\cdot\mathbf{r}}d\mathbf{K} , \quad (1)$$

where $\mathbf{K}$ is a wave vector in the Fourier space and

$$\Delta V(\mathbf{K})=\sum_{\mathbf{K}'}\epsilon_H^{-1}(\mathbf{K},\mathbf{K}')\Delta V^b(\mathbf{K}') , \quad (2)$$

where $\epsilon_H^{-1}(\mathbf{K},\mathbf{K}')$ is the inverse dielectric tensor of the host metal. $\Delta V^b(\mathbf{K})$ is unscreened excess impurity potential defined as

$$\Delta V^b(\mathbf{K})=V_I^b(\mathbf{K})-V_H^b(\mathbf{K}) , \quad (3)$$

where $V_I^b(\mathbf{K})$ and $V_H^b(\mathbf{K})$ are bare-ion potential for the impurity and host ions. Solving the Poisson equation for $\Delta V(\mathbf{K})$ one finds

$$\Delta n(\mathbf{K})=\frac{1}{v(\mathbf{K})}\sum_{\mathbf{K}'}[\epsilon_H^{-1}(\mathbf{K},\mathbf{K}')-\delta_{\mathbf{K},\mathbf{K}'}]\Delta V^b(\mathbf{K}') , \quad (4)$$

where

$$v(\mathbf{K})=\frac{4\pi e^2}{K^2}[1-f_{\rm xc}(\mathbf{K})] \quad (5)$$

is the Fourier transform of electron-electron interaction potential and the function $f_{\rm xc}(\mathbf{K})$ takes care of the exchange and correlation interactions.

The general expression for the dielectric tensor is[13]

$$\epsilon_H(\mathbf{K},\mathbf{K}')=\delta_{\mathbf{K}\mathbf{K}'}-v(\mathbf{K})\chi_H(\mathbf{K},\mathbf{K}') , \quad (6)$$

where the polarizability function

$$\chi_H(\mathbf{K},\mathbf{K}')=\sum_{\lambda,\lambda'}\sum_{\mathbf{K}'',\mathbf{k}}\left[\frac{f_0(E_{\mathbf{k}}^{\lambda})-f_0(E_{\mathbf{k}+\mathbf{K}''}^{\lambda'})}{E_{\mathbf{k}}^{\lambda}-E_{\mathbf{k}+\mathbf{K}''}^{\lambda'}}\right]\times\langle\psi_{\mathbf{k}}^{\lambda}(\mathbf{r})\,|\,e^{-i\mathbf{K}\cdot\mathbf{r}}\,|\,\psi_{\mathbf{k}+\mathbf{K}''}^{\lambda'}(\mathbf{r})\rangle\times\langle\psi_{\mathbf{k}+\mathbf{K}''}^{\lambda'}(\mathbf{r})\,|\,e^{i\mathbf{K}'\cdot\mathbf{r}}\,|\,\psi_{\mathbf{k}}^{\lambda}(\mathbf{r})\rangle . \quad (7)$$

Here $f_0(E_{\mathbf{k}}^{\lambda})$ is Fermi-Dirac function. $E_{\mathbf{k}}^{\lambda}$ is the energy eigenvalue of the state $|k\lambda\rangle$, $\psi_{\mathbf{k}}^{\lambda}(\mathbf{r})=\langle\mathbf{r}\,|\,\mathbf{k}\lambda\rangle$ and λ is band index which represents principal, orbital, and magnetic quantum numbers. $\chi_H(\mathbf{K},\mathbf{K}')$ is a product of band structure part (in large brackets) and overlap matrix element part. The periodicity of the electronic charge distribution requires $\epsilon_H(\mathbf{K},\mathbf{K}')$ to be nonzero when $\mathbf{K}'=\mathbf{K}+\mathbf{G}$, where $\mathbf{G}$ is a reciprocal lattice vector. Thus Eqs. (2) and (4) may be rewritten as

$$\Delta V(\mathbf{K})=\sum_{\mathbf{G}}\epsilon_H^{-1}(\mathbf{K},\mathbf{K}+\mathbf{G})\Delta V^b(\mathbf{K}+\mathbf{G}) , \quad (8)$$

and

$$\Delta n(\mathbf{K})=\frac{1}{v(\mathbf{K})}\sum_{\mathbf{G}}[\epsilon_H^{-1}(\mathbf{K},\mathbf{K}+\mathbf{G})-\delta_{\mathbf{K},\mathbf{K}+\mathbf{G}}]\times\Delta V^b(\mathbf{K}+\mathbf{G}) . \quad (9)$$

$\Delta n(\mathbf{K})$ and $\Delta V(\mathbf{K})$ can be evaluated if one is able to find $\epsilon_H^{-1}(\mathbf{K},\mathbf{K}+\mathbf{G})$. If one uses the localized representation for $\psi_{\mathbf{k}}^{\lambda}(\mathbf{r})$, the band structures and overlap parts of $\epsilon_H(\mathbf{K},\mathbf{K}+\mathbf{G})$ are factorized, making the $\epsilon_H^{-1}(\mathbf{K},\mathbf{K}+\mathbf{G})$ tractable. We adopt two schemes to calculate $\epsilon_H(\mathbf{K},\mathbf{K}+\mathbf{G})$, (i) the LCAO approximation and (ii) mixed-band-structure scheme.

A. LCAO approximation

The wave function $\psi_{\mathbf{k}}^{\lambda}(\mathbf{r})$ in the LCAO scheme is

$$\psi_{\mathbf{k}}^{\lambda}(\mathbf{r})=\frac{1}{\sqrt{N}}\sum_n e^{i\mathbf{k}\cdot\mathbf{R}_n}\phi_{\lambda}(\mathbf{r}-\mathbf{R}_n) , \quad (10)$$

where $\phi_{\lambda}(\mathbf{r}-\mathbf{R}_n)$ is the atomic wave function at site $\mathbf{R}_n$ and the sum is over all the N lattice sites in the crystal space. $\phi_{\lambda}(\mathbf{r}-\mathbf{R}_n)$ may also be taken as Wannier function centered on the site $\mathbf{R}_n$. Using Eq. (10) in (7) we find

$$\chi_H(\mathbf{K},\mathbf{K}+\mathbf{G})=\sum_{n,n'}\sum_{\lambda\lambda'}A_{n\lambda\lambda'}(\mathbf{K})f_{n\lambda\lambda',n'\lambda\lambda'}(\mathbf{K})\times A_{n'\lambda\lambda'}^{*}(\mathbf{K}+\mathbf{G}) , \quad (11)$$

where

$$A_{n\lambda\lambda'}(\mathbf{K})=\int\phi_{\lambda}^{*}(\mathbf{r})e^{-i\mathbf{K}\cdot\mathbf{r}}\phi_{\lambda'}(\mathbf{r}+\mathbf{R}_n)d\mathbf{r} , \quad (12)$$

and

$$f_{n\lambda\lambda',n'\lambda\lambda'}(\mathbf{K})=\sum_{\mathbf{k}\le\mathbf{k}_F}\frac{f_0(E_{\mathbf{k}}^{\lambda})-f_0(E_{\mathbf{k}+\mathbf{K}}^{\lambda'})}{E_{\mathbf{k}}^{\lambda}-E_{\mathbf{k}+\mathbf{K}}^{\lambda'}}\times e^{-i(\mathbf{k}+\mathbf{K})\cdot(\mathbf{R}_n-\mathbf{R}_{n'})} . \quad (13)$$

The inverse dielectric matrix is calculated using Eq. (11) in Eq. (6). The result is[4]

$$\epsilon_H^{-1}(\mathbf{K},\mathbf{K}+\mathbf{G})=\delta_{\mathbf{K},\mathbf{K}+\mathbf{G}}+v(\mathbf{K})\sum_{p,p'}A_p(\mathbf{K})F_{pp'}(\mathbf{K})A_{p'}^{*}(\mathbf{K}+\mathbf{G}) , \quad (14)$$

where

$$F_{pp'}(\mathbf{K})=\left[f_{pp'}^{-1}(\mathbf{K})-\sum_{\mathbf{G}'}A_{p'}^{*}(\mathbf{K}+\mathbf{G}')A_p(\mathbf{K}+\mathbf{G}')\times v(\mathbf{K}+\mathbf{G}')\right]^{-1} . \quad (15)$$

The subscript $p\equiv\{n\lambda\lambda'\}$. The second term of Eq. (14) is the contribution due to multipole character of the polarization of charge at the lattice positions. The intraband ($\lambda=\lambda'$) transitions in the various subbands produce monopoles while the interband ($\lambda\neq\lambda'$) transitions produce dipoles at the atomic sites with form factor $A_p(\mathbf{K})$. Therefore, the second term of Eq. (14) includes contributions arising from monopole-monopole, monopole-dipole, dipole-monopole, and dipole-dipole interactions mediated by the resonant function $F_{pp'}(\mathbf{K})$. Thus Eq. (14) describes the screening similar to that of a dipolar model for insulators.[4,5]

$\Delta V(\mathbf{K})$ and $\Delta n(\mathbf{K})$ are obtained by substituting Eq. (14) in Eqs. (8) and (9). One gets

$$\Delta V(\mathbf{K})=\Delta V^b(\mathbf{K})+\sum_{\mathbf{G}}\sum_{p'}W_{p'}(\mathbf{K})X_{p'}(\mathbf{K}+\mathbf{G}) \quad (16)$$

and

$$\Delta n(\mathbf{K})=\sum_{\mathbf{G}}\sum_{p'}Y_{p'}(\mathbf{K})X_{p'}(\mathbf{K}+\mathbf{G}) , \quad (17)$$

where

$$X_{p'}(\mathbf{K})=A_{p'}^{*}(\mathbf{K})\Delta V^{b}(\mathbf{K}) , \tag{18}$$

$$Y_{p'}(\mathbf{K})=\sum_{p} A_{p}(\mathbf{K})F_{pp'}(\mathbf{K}) , \tag{19}$$

$$W_{p'}(\mathbf{K})=v(\mathbf{K})\sum_{p} A_{p}(\mathbf{K})F_{pp'}(\mathbf{K}) . \tag{20}$$

$\Delta V(\mathbf{r})$ in r space is obtained using the identity

$$\sum_{n} u(\mathbf{R}_n)e^{i\mathbf{K}\cdot\mathbf{R}_n}=\sum_{\mathbf{G}} u(\mathbf{K}+\mathbf{G}) . \tag{21}$$

This gives

$$\Delta V(\mathbf{r})=\Delta V^{b}(\mathbf{r})+\sum_{n}\sum_{p'} X_{p'}(\mathbf{R}_n)W_{p'}(\mathbf{r}-\mathbf{R}_n) , \tag{22}$$

where

$$X_{p'}(\mathbf{R}_n)=\frac{1}{(2\pi)^3}\int X_{p'}(\mathbf{K})e^{i\mathbf{K}\cdot\mathbf{R}_n}d\mathbf{K} , \tag{23}$$

$$W_{p'}(\mathbf{r}-\mathbf{R}_n)=\frac{1}{(2\pi)^3}\int W_{p'}(\mathbf{K})e^{i\mathbf{K}\cdot(\mathbf{r}-\mathbf{R}_n)}d\mathbf{K} . \tag{24}$$

Here $X_{p'}(\mathbf{r})$ and $W_{p'}(\mathbf{r})$ are the Fourier transforms of $X_{p'}(\mathbf{K})$ and $W_{p'}(\mathbf{K})$. Similarly one can get the expression for $\Delta n(\mathbf{r})$ by taking the Fourier transform of $\Delta n(\mathbf{K})$ given by Eq. (17) and using the identity (21). It gives

$$\Delta n(\mathbf{r})=\sum_{n}\sum_{p'} X_{p'}(\mathbf{R}_n)Y_{p'}(\mathbf{r}-\mathbf{R}_n) , \tag{25}$$

where $Y_{p'}(\mathbf{r})$ is the Fourier transform of $Y_{p'}(\mathbf{K})$, Here Eqs. (22) and (25) are exact in the LCAO approximation. The first term in Eq. (22) is the unscreened excess impurity potential. The screening effects due to the s and d electrons of the host metal are combined in the second term. Therefore in this scheme it is not possible to compare the contributions to $\Delta V(\mathbf{r})$ and $\Delta n(\mathbf{r})$ from the s and d bands separately.

B. Mixed band scheme

In the TM's it is suitable for all practical purposes, to use an orthogonalized plane wave representation for the s-electron states and the localized representation for the d-electron states. In this combined band structure scheme, the dielectric matrix is split up in two parts; first is the diagonal part $\epsilon_0(\mathbf{K})$ arising from the intraband transitions in the s band and is just the Lindhard function. The second contribution arises from the intraband and interband transitions between the partially filled s and d subbands and contains both the diagonal and nondiagonal contribution. Therefore, in the RPA, $\epsilon_H(\mathbf{K},\mathbf{K}+\mathbf{G})$ can be written as

$$\epsilon_H(\mathbf{K},\mathbf{K}+\mathbf{G})=\epsilon_0(\mathbf{K})\delta_{\mathbf{K},\mathbf{K}+\mathbf{G}} -v(\mathbf{K})\sum_{s,s'} A_s(\mathbf{K})f_{ss'}(\mathbf{K})A_{s'}^{*}(\mathbf{K}+G) , \tag{26}$$

where

$$A_s(\mathbf{K})=\int \phi_{l\lambda}^{*}(\mathbf{r})\exp(-i\mathbf{K}\cdot\mathbf{r})\phi_{l\lambda'}(\mathbf{r}+\mathbf{R}_n)d\mathbf{r} , \tag{27}$$

$$f_{ss'}(\mathbf{K})=\sum_{\mathbf{k}\le\mathbf{k}_F}\frac{f_0(E_{\mathbf{k}}^{l\lambda})-f_0(E_{\mathbf{k}+\mathbf{K}}^{l\lambda'})}{E_{\mathbf{k}}^{l\lambda}-E_{\mathbf{k}+\mathbf{K}}^{l\lambda'}} \times\exp[-i(\mathbf{k}+\mathbf{K})\cdot(\mathbf{R}_n-\mathbf{R}_{n'})] . \tag{28}$$

The subscript s denotes $\{l\lambda\lambda'\}$, l is orbital quantum number. The symbol for the subscript is changed as there are different transitions in this scheme. The inverse dielectric matrix is obtained as described earlier and is given as

$$\epsilon_H^{-1}(\mathbf{K},\mathbf{K}+\mathbf{G}) =\frac{1}{\epsilon_0(\mathbf{K}+\mathbf{G})} \times\left[\delta_{\mathbf{K},\mathbf{K}+\mathbf{G}} +\frac{v(\mathbf{K})}{\epsilon_0(\mathbf{K})}\sum_{s,s'} A_s(\mathbf{K})F_{ss'}(\mathbf{K})A_{s'}^{*}(\mathbf{K}+\mathbf{G})\right] \tag{29}$$

where

$$F_{ss'}(\mathbf{K})=[f_{ss'}^{-1}(\mathbf{K})-f_{ss'}^{d}(\mathbf{K})]^{-1} =\left[f_{ss'}^{-1}(\mathbf{K})-\sum_{\mathbf{G}'} A_s(\mathbf{K}+\mathbf{G}')A_{s'}^{*}(\mathbf{K}+\mathbf{G}') \times\frac{v(\mathbf{K}+\mathbf{G}')}{\epsilon_0(\mathbf{K}+\mathbf{G}')}\right]^{-1} . \tag{30}$$

In this model, polarization of d-electron charge produces monopoles and dipoles at the lattice positions which are screened by the s conduction electrons.[14] This is similar to the screened breathing shell model.[14] For the intraband transitions $A_s(\mathbf{K})/\epsilon_0(\mathbf{K})$ gives the screened form factor for the monopoles, while for the interband transitions it gives the screened from factor for the dipoles. Putting $\epsilon_0(\mathbf{K})=1$ for ideal insulators, Eq. (29) gives screened dipolar model of screening.[15] Equation (29) includes all shorts of interactions between the screened monopoles and dipoles, mediated by $F_{ss'}(\mathbf{K})$, as discussed earlier.

Substituting Eq. (29) in Eqs. (8) and (9), we get

$$\Delta V(\mathbf{K})=\Delta V^{0}(\mathbf{K})+\sum_{s'}\sum_{\mathbf{G}} T_{s'}(\mathbf{K})U_{s'}(\mathbf{K}+\mathbf{G}) \tag{31}$$

and

$$\Delta n(\mathbf{K})=\Delta n^{0}(\mathbf{K})+\sum_{s'}\sum_{G} S_{s'}(\mathbf{K})U_{s'}(\mathbf{K}+\mathbf{G}) , \tag{32}$$

where

$$\Delta V^{0}(\mathbf{K})=\Delta V^{b}(\mathbf{K})/\epsilon_0(\mathbf{K}) , \tag{33}$$

$$\Delta n^{0}(\mathbf{K})=\frac{1}{v(\mathbf{K})}\left[\frac{1}{\epsilon_0(\mathbf{K})}-1\right]\Delta V^{b}(\mathbf{K}) , \tag{34}$$

$$T_{s'}(\mathbf{K})=v(\mathbf{K})\sum_{s}\frac{A_s(\mathbf{K})}{\epsilon_0(\mathbf{K})}F_{ss'}(\mathbf{K}) , \tag{35}$$

$$S_{s'}(\mathbf{K})=\sum_{s}\frac{A_s(\mathbf{K})}{\epsilon_0(\mathbf{K})}F_{ss'}(\mathbf{K}) , \tag{36}$$

$$U_{s'}(\mathbf{K}+\mathbf{G})=\Delta V^b(\mathbf{K}+\mathbf{G})\frac{A_{s'}^*(\mathbf{K}+\mathbf{G})}{\epsilon_0(\mathbf{K}+\mathbf{G})} . \tag{37}$$

$\Delta V(\mathbf{r})$ and $\Delta n(\mathbf{r})$ can be obtained by taking the Fourier transforms of Eqs. (31) and (32) and using Eq. (21). The final expressions are

$$\Delta V(\mathbf{r})=\Delta V^0(\mathbf{r})+\sum_{s'}\sum_{n}U_{s'}(\mathbf{R}_n)T_{s'}(\mathbf{r}-\mathbf{R}_n) , \tag{38}$$

and

$$\Delta n(\mathbf{r})=\Delta n^0(\mathbf{r})+\sum_{s'}\sum_{n}U_{s'}(\mathbf{R}_n)S_{s'}(\mathbf{r}-\mathbf{R}_n) . \tag{39}$$

$\Delta V^0(\mathbf{r})$, $\Delta n^0(\mathbf{r})$, $U_s(\mathbf{r})$, $T_S(\mathbf{r})$, and $S_s(\mathbf{r})$ are the Fourier transforms of $\Delta V^0(\mathbf{K})$, $\Delta n^0(\mathbf{K})$, $U_s(\mathbf{K})$, $T_s(\mathbf{K})$, and $S_s(\mathbf{K})$, respectively. Here again Eqs. (38) and (39) are the exact expressions in the combined band structure scheme. The first term in Eqs. (38) and (39) is isotropic and corresponds to the simple metallike contribution. The second term is anisotropic in nature and gives the d-band contribution. The anisotropy in $\Delta V(\mathbf{r})$ and $\Delta n(\mathbf{r})$ is caused by the band structure of the host metal, through $T_s(\mathbf{K})$ and $S_s(\mathbf{K})$ and by the lattice sum. These facts make $\Delta V(\mathbf{r})$ and $\Delta n(\mathbf{r})$ dependent on the crystal structure of the dilute alloy.

III. CALCULATIONS AND RESULTS

A. The change in potential $\Delta V(\mathbf{r})$ and charge density $\Delta n(\mathbf{r})$

The exact calculations of the EFG using Eq. (25) are nontrivial as they involve the full band structure calculations. Therefore, we calculate $\Delta V(\mathbf{r})$, $\Delta n(\mathbf{r})$, and the EFG in the mixed band scheme where the numerical computations are tractable in model band structure. This will enable us to estimate the effect of local fields on $\Delta V(\mathbf{r})$, $\Delta n(\mathbf{r})$, and EFG's. We assume $\Delta V^0(\mathbf{K})$, $\Delta n^0(\mathbf{K})$, $T_s(\mathbf{K})$, $S_s(\mathbf{K})$, and $U_s(\mathbf{K})$ to all be isotropic, i.e., $|\mathbf{K}|$ dependent only. This is not rigorously true for $T_s(\mathbf{K})$ and $S_s(\mathbf{K})$ since they invole the electronic band structure through $F_{ss'}(\mathbf{K})$, which is not isotropic but periodic. $T_s(\mathbf{K})$ and $S_s(\mathbf{K})$ become isotropic if the average value of $F_{ss'}(\mathbf{K})$, denoted by $\langle F_{ss'}(\mathbf{K})\rangle$, is substituted. Further, $\langle F_{ss'}(\mathbf{K})\rangle$ is obtained by substituting the average values of $f_{ss'}(\mathbf{K})$ and $f^d_{ss'}(\mathbf{K})$. In this approximation $\Delta V(\mathbf{r})$ and $\Delta n(\mathbf{r})$ are given as

$$\Delta V(\mathbf{r})=\Delta V^0(|\mathbf{r}|)+\sum_{s'}\sum_{n}U_{s'}(|\mathbf{R}_n|)T_{s'}(|\mathbf{r}-\mathbf{R}_n|) , \tag{40}$$

$$\Delta n(\mathbf{r})=\Delta n^0(|\mathbf{r}|)+\sum_{s'}\sum_{n}U_{s'}(|\mathbf{R}_n|)S_{s'}(|\mathbf{r}-\mathbf{R}_n|) . \tag{41}$$

Here essentially the anisotropy due to band structure effects is averaged out. The anisotropy due to lattice sum is retained through the second term of Eqs. (40) and (41).

The formalism of combined band structure scheme is applied to calculate $\Delta V(\mathbf{r})$, $\Delta n(\mathbf{r})$, and the EFG for dilute V alloys: VMn, VNb, and VTa with $3d$, $4d$, and $5d$ TM impurities, respectively. To evaluate $\Delta V(\mathbf{r})$ and $\Delta n(\mathbf{r})$ one needs $\Delta V^b(\mathbf{K})$ and $\epsilon_H(\mathbf{K},\mathbf{K}+\mathbf{G})$. $\Delta V^b(\mathbf{K})$ [given by Eq. (3)] is estimated using the Heine-Abarenkov–type transition-metal model potential for both the host and impurity ions.[16] The impurity produces dilation in the host matrix, leading to change in the impurity valency. Therefore, the normal valency of the impurity is replaced by Blatt corrected impurity valency.[8]

The dielectric matrix $\epsilon_H(\mathbf{K},\mathbf{K}+\mathbf{G})$ for V metal is evaluated in the isotropic noninteracting band scheme of Singh *et al.*,[5] where s electrons are represented by the plane waves and the d electrons by the tight binding wave functions. According to isotropic and noninteracting band structure, V metal has valency 3; its s band and the two d subbands are partially filled, one d subband is completely filled, and the remaining two d subbands are empty and above Fermi energy. In computing the dielectric matrix, two types of transitions are considered; (i) intraband transitions in the partially filled s and d subbands and (ii) interband transitions from filled and partially filled d subbands to partially filled s and d subbands. It has been found that contribution of interband transitions to the dielectric matrix is very small as compared to that of intraband transitions.[5]

The overlap between the d atomic orbitals $\phi_{dm}(\mathbf{r}-\mathbf{R}_n)$ at different lattice sites is neglected and the hybridization between the different d subbands is included by giving equal weight to the d subbands with different m values. In these approximations $A_s(\mathbf{K})$ and $f_{ss'}(\mathbf{K})$ become independent of the subscript s. The functions $\epsilon_0(\mathbf{K})$, $A(\mathbf{K})$, and $f(\mathbf{K})$ become isotropic in the noninteracting band scheme and are given as[5]

$$\epsilon_0(\mathbf{K})=1+\frac{2m_s k_{fs}e^2}{\pi^2\hbar^2}[1-f_{\mathrm{xc}}(\mathbf{K})] \times\left[1+\frac{4k_{fs}^2-|\mathbf{K}|^2}{4k_{fs}|\mathbf{K}|}\ln\left|\frac{2k_{fs}+|\mathbf{K}|}{2k_{fs}-|\mathbf{K}|}\right|\right] , \tag{42}$$

$$f(\mathbf{K})=-\frac{1}{2\pi^2\hbar^2}\sum_i m_{di}k_{fdi} \times\left[1+\frac{4k_{fdi}^2-|\mathbf{K}|^2}{4_{fdi}^k|\mathbf{K}|}\times\ln\left|\frac{2k_{fdi}+|\mathbf{K}|}{2k_{fdi}-|\mathbf{K}|}\right|\right] , \tag{43}$$

and

$$A(\mathbf{K})=\int_0^\infty j_0(|\mathbf{K}|r)R_{3d}^2(r)dr . \tag{44}$$

Here m_s and k_{fs} are the effective mass and Fermi momentum of the s band and m_{di} and k_{fdi} are the corresponding quantities for the ith partially filled d subband. $R_{3d}(r)$ is the radial wave function for the $3d$ electrons and $j_0(|\mathbf{K}|r)$ is the zeroth-order spherical Bessel function.

In evaluating the dielectric matrix, Hubbard-type exchange and correlation corrections are included in the electron-electron interaction potential. The function $f^d(\mathbf{K})$, in Eq. (30), is anisotropic; therefore its values are evaluated for the V metal along the principal symmetry directions [100], [110], and [111]. It is found that $f^d(\mathbf{K})$ is nearly the same along these directions for $|\mathbf{K}| \leq 8$ a.u. For large values of $|\mathbf{K}|$, $f^d(\mathbf{K})$ decreases rapidly to zero. Therefore, the average value of $f^d(\mathbf{K})$ is obtained by taking the simple average of its values along [100], [110], and [111] directions. Using this in Eq. (30), the average value of function $F(\mathbf{K})$, symbolized by $\langle F(\mathbf{K})\rangle$ is calculated for the V metal and is shown in Fig. 1. $\langle F(\mathbf{K})\rangle$ exhibits a weak peak at small $|\mathbf{K}|$ which is due to the resonant form of $F(\mathbf{K})$.

$\Delta V(\mathbf{r})$ and $\Delta n(\mathbf{r})$ are calculated from Eqs. (40) and (41) for dilute alloys *V*Mn, *V*Nb, and *V*Ta. The model potential parameters for TM impurities are taken from Animalu[16] while those for the host V metal are taken from Singh *et al.*,[5] as these reproduce phonon frequencies of V quite reasonably in the noninteracting band scheme. To achieve convergence over the integrals involving $\Delta V^b(\mathbf{K})$ we have applied the damping factor to the TM model potential as suggested by Animalu and Heine.[17] Figure 2 shows $\Delta V(\mathbf{r})$ versus $\mathbf{r}$ along the [100] direction for *V*Mn, *V*Nb, and *V*Ta. Figure 3 shows $\Delta n(\mathbf{r})$ along the [100] direction for *V*Ta only and the behavior of $\Delta n(\mathbf{r})$ for *V*Nb and *V*Mn is similar to that of *V*Ta.

It is evident from Figs. 2 and 3 that $\Delta V(\mathbf{r})$ and $\Delta n(\mathbf{r})$ are large near the impurity and decrease fast, exhibiting the usual Friedel oscillations at large distances from the impurity. The large values of $\Delta V(\mathbf{r})$ and $\Delta n(\mathbf{r})$ at or near the impurity site are due to the resonant scattering of the conducting electrons from the TM impurity. The rapid decrease is due to the large screening of the impurity by the *d* electrons of V metal. This conclusion is consistent with the small wipeout numbers observed in dilute V alloys with TM impurities.[6] The magnitudes of $\Delta V(\mathbf{r})$ and $\Delta n(\mathbf{r})$ are small at the first nearest neighbor (1NN) and beyond but these are oscillatory in nature. It shows that

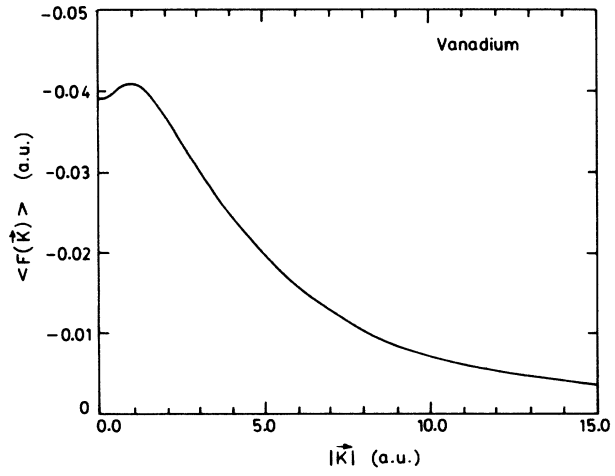

FIG. 1. $\langle F(\mathbf{K})\rangle$, in a.u., as a function of $|\mathbf{K}|$ for V metal.

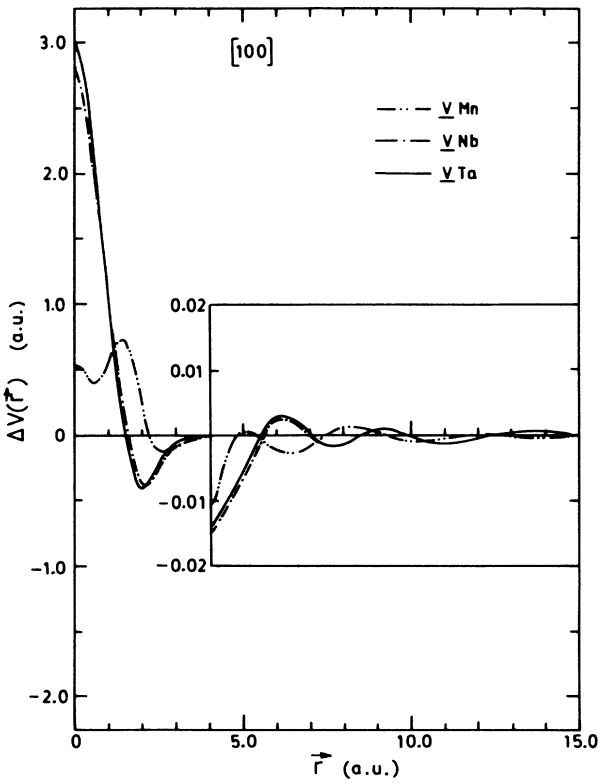

FIG. 2. $\Delta V(\mathbf{r})$ vs $\mathbf{r}$ along the [100] direction for *V*Mn, *V*Nb, and *V*Ta alloys.

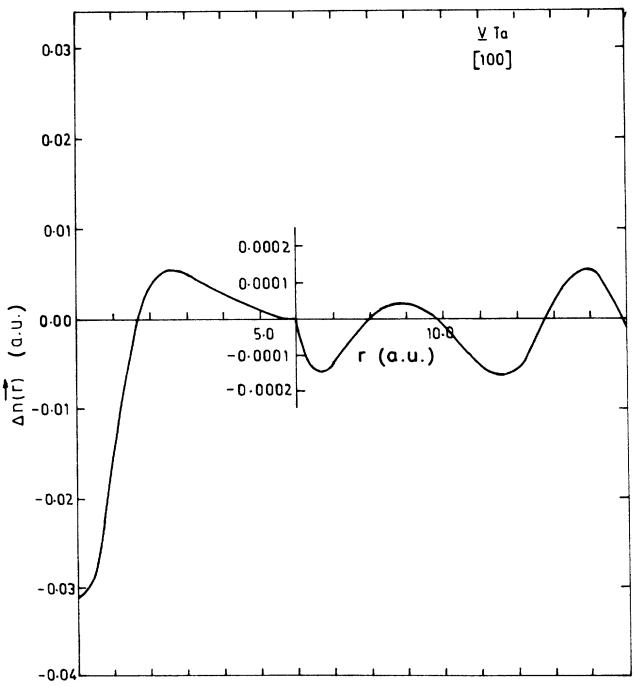

FIG. 3. $\Delta n(\mathbf{r})$ vs $\mathbf{r}$ along the [100] direction for *V*Ta alloy.

TABLE I. The calculated values of the EFG (10^{24} cm^{-3}) at the 1NN site of impurity with coordinates $(a/2)$ [111] along with q_{expt} for VMn, VNb, and VTa.

Alloy	Contributions to $q_{\parallel}^{v}$ Isotropic	Anisotropic	$q_{\parallel}^{v}$	$q_{\parallel}^{s}$	$\lvert q_{\text{calc}} \rvert$	q_{expt}
VMn	−0.735	−0.182	−0.917	0.280	0.637	0.74
VNb	0.112	−0.325	−0.213	−0.805	1.019	0.84
VTa	0.155	−0.308	−0.153	−0.798	0.951	1.00

the impurity is not completely screened within its Wigner-Seitz cell. In spite of large screening the impurity has extended interaction with the neighboring host atoms. This conclusion is consistent with the calculations of Podloucky *et al.*[18]

It is evident from Fig. 2 that $|\Delta V(\mathbf{r})|$ for VMn is smallest as compared to that for VNb and VTa. It is due to the fact that the excess impurity charge $\Delta Z = Z_I - Z_H$ on Mn impurity is 1, while it is 2 for Nb and Ta impurities. The contribution to $\Delta V(\mathbf{r})$ and $\Delta n(\mathbf{r})$ due to the LF's is 10–20 % in these alloys. The second terms in Eqs. (40) and (41) contribute for the interactions between the screened monopoles and dipoles induced at the lattice positions. These contributions are found to decrease rapidly away from the impurity, therefore, only a few nearest neighbhors of the impurity contributed significantly towards the LF's. The isotropic condition on the functions $T(\mathbf{K})$, $S(\mathbf{K})$, and $U(\mathbf{K})$ reduced the anisotropy in $\Delta V(\mathbf{r})$ and $\Delta n(\mathbf{r})$.

B. The EFG

The EFG due to an impurity consists of two contributions. First is the valence EFG q^v arising due to the scattering of the conduction electrons from the excess charge on the impurity. In cubic metallic alloys q^v is a cylindrically symmetric traceless tensor and its principal component is along the line joining the host and impurity atoms usually called the parallel ($\parallel$) direction. Taking the Z axis along the parallel direction, the principal component of the valence EFG $q_{\parallel}^{v}$ is expressed as[8]

$$q_{\parallel}^{v}(\mathbf{r}) = \tfrac{2}{3}[1-\gamma(\mathbf{r})]\left[\frac{d^2}{dr^2}\Delta V(\mathbf{r}) - \frac{1}{r}\frac{d}{dr}\Delta V(\mathbf{r})\right] . \tag{45}$$

Here $\gamma(\mathbf{r})$ is the Sternheimer antishielding factor that accounts for core polarization of the host atom at which the EFG is to be evaluated. $\gamma(\mathbf{r})$ acquires a constant saturated value outside the core region, therefore, we use the asymptotic value of $\gamma(\mathbf{r})$ denoted as γ_∞ and it is -11 for V metal.

The second contribution to the EFG, called the size effect, is due to the different size and electronic structure of the impurity atom. The impurity produces strain field in the host lattice and the neighboring host ions are displaced. The dilation changes the effective charge on the impurity; therefore, Blatt-corrected impurity valency is used in evaluating $q_{\parallel}^{v}(\mathbf{r})$ and these are calculated at the displaced positions of the nearest neighbors. The displacement is estimated using spherically symmetric strain field in the elastic continuum limit.[19] The direct size EFG q^s arises due to strain-field-induced redistribution of the conduction electrons. We[7] proposed a formalism for q^s for dilute alloys with bcc structure and its principal component q^s at the 1NN site in the parallel direction is expressed[7] as

$$q_{\parallel}^{s} = -3a^3\left[\frac{1}{a}\frac{da}{dc}\right]\frac{C_s F_{44}}{2\pi v_E d_1^3} , \tag{46}$$

where F_{11}, F_{12}, and F_{44} are nonzero elements of fourth-order tensor $\overleftrightarrow{F}$ for a cubic system and are evaluated using the screened point charge model. C_s is the size strength parameter.[20]

$q_{\parallel}^{v}$ and $q_{\parallel}^{s}$ are calculated at the displaced positions of the 1NN site of impurity with coordinates $(a/2)$ (111) and these are added to obtain the total EFG q_{calc}. These results are given in Table I along with the experimental values of the EFG q_{expt} from Meerwall and Rowland.[6] The contributions to $q_{\parallel}^{v}$ from isotropic and anisotropic $\Delta n(\mathbf{r})$ are tabulated separately. The anisotropic contribution due to the LF's is significant in VMn and rather dominating the VNb and VTa alloys. Although the magnitude of the LF contribution is small, it is oscillatory in character. As evident from Eq. (45) $q_{\parallel}^{v}$ is related to first and second derivatives of $\Delta V(\mathbf{r})$; therefore, $q_{\parallel}^{v}$ becomes very sensitive to the LF contribution towards $\Delta V(\mathbf{r})$. The isotropic and anisotropic contributions to the EFG have the same sign in VMn but have opposite signs in VNb and VTa.

The smaller values of $q_{\parallel}^{v}$ show that the valence effect alone cannot explain the measured values q_{expt}. In estimating $q_{\parallel}^{s}$ the value of C_s is taken to be 7, which gives reasonable agreement between $|q_{\text{calc}}|$ and q_{expt} for VTa and the same value is used in calculating $|q_{\text{calc}}|$ for alloys VMn and VNb. $|q_{\text{calc}}|$ agrees reasonably well with q_{expt} for these alloys. The comparison shows that $q_{\parallel}^{s}$ dominates $q_{\parallel}^{v}$ in VNb and VTa while the reverse is found in VMn. Therefore both the valence and size effect contributions are important to explain q_{expt}. This conclusion is in contrast to the prediction of Von Meerwall and Rowland,[6] who predicted from the linear relation between the EFG and $a^{-1}(da/dc)$ that the EFG arises mainly due to the size effect. Further, the principal component of EFG tensor is along the parallel direction, which is consistent with the nuclear magnetic resonance (NMR) observations.[2,6]

IV. CONCLUSIONS

The dielectric screening theory gives exact expressions for $\Delta V(\mathbf{r})$ and $\Delta n(\mathbf{r})$ in the crystal space, in both the LCAO approximation and the combined band structure

representation. The novel feature of the combined band structure representation is that the isotropic and anisotropic contributions are separable and the latter is the manifestation of the LF effects. If one neglects the d-band effects the conventional dielectric screening formalism of simple metals is retrieved.[21] The numerical results for $\Delta V(\mathbf{r})$, $\Delta n(\mathbf{r})$, and the EFG establish the importance of the LF's in the TM-based dilute alloys which were neglected in earlier calculations.[8,19]

The present theory for dilute TM alloys with TM impurities has the following advantages over the partial wave method. (i) The dielectric screening theory yields expressions for $\Delta V(\mathbf{r})$, $\Delta n(\mathbf{r})$, and the EFG valid at all distances from the impurity, in contrast to the asymptotic nature of partial wave analysis.[2] (ii) The present approach is free from all the deficiencies involved in calculating the phase shifts, occurring in the partial wave analysis, particularly in alloys with TM impurities.[7] (iii) The dielectric screening theory in conjunction with the pseudopotential approach includes the Bloch character of s, p, and d bands for conduction electrons in the evaluation of $\Delta V(\mathbf{r})$, $\Delta n(\mathbf{r})$, and the EFG through the use of the TM model potential for both the host and impurity atoms and through the dielectric tensor of the host metal. On the other hand, in the partial wave method the Bloch character is introduced in the calculation of the EFG through a core enhancement parameter. (iv) The d potential-well-depth $A_2(E) \propto (E - E^d)^{-1}$ is strongly dependent on energy and represents s-d hybridization analogous to that found in the orthogonalized plane wave pseudopotential theory.[3] Such a resonance behavior is responsible for the existence of a virtual bound state under favorable circumstances.[1,2] The exchange corrections take care of the nonlinear screening effects to some extent.

In conclusion we mention that we have made an attempt to incorporate full dielectric tensor for impurity screening and in estimating EFG's for dilute transitional cubic alloys.

ACKNOWLEDGMENTS

We thank Professor S. K. Sinha for fruitful discussions and Professor S. K. Joshi for helpful suggestions.

[1] J. Friedel, Can. J. Phys. **34**, 1190 (1956).
[2] G. Gruner and M. Minier, Adv. Phys. **26**, 231 (1977).
[3] W. A. Harrison, Phys. Rev. **181**, 1036 (1969).
[4] W. Hanke, Phys. Rev. B **8**, 4585 (1973); **8**, 4591 (1973).
[5] J. Singh, N. Singh, and S. Prakash, Phys. Rev. B **18**, 2954 (1978).
[6] E. Von Meerwall and T. J. Rowland, Phys. Rev. B **5**, 2480 (1972).
[7] B. Pal, J. Singh, S. D. Raj, and S. Prakash, Phys. Status Solidi B **129**, 301 (1985).
[8] S. K. Rattan, S. Prakash, and J. Singh, Phys. Lett. **114A**, 279 (1986).
[9] F. Stern, Phys. Rev. Lett. **6**, 675 (1961).
[10] T. L. Loucks, *Augmented Plane Wave Method* (Benjamin, New York, 1967).
[11] A. Seeger and E. Mann, in Proceedings of National Bureau of Standards Conference, Washington, 1967 (unpublished).
[12] P. Rennert, Phys. Status Solidi **50**, K37 (1972).
[13] L. J. Sham and J. Ziman, Solid State Physics (Academic, New York, 1963), Vol. 15, p. 221.
[14] U. Schröder, Solid State Commun. **4**, 347 (1966); U. Schröder and V. Nusslein, Phys. Status Solidi **21**, 309 (1967).
[15] W. Hanke, in *Phonons*, edited by M. Nusimovici (Flammarion, Paris, 1971), p. 296.
[16] A. O. E. Animalu, Phys. Rev. B **18**, 3542 (1973).
[17] A. O. E. Animalu and V. Heine, Philos. Mag. **12**, 1249 (1965).
[18] R. Podloucky, J. Deutz, R. Zeller, and P. H. Dederichs, Phys. Status Solidi B **112**, 515 (1982).
[19] J. Singh, S. K. Rattan, B. Pal, and S. Prakash, Physica B + C **144B**, 368 (1987).
[20] E. A. Faulkner, Philos. Mag. **5**, 843 (1960).
[21] Y. Fukai and W. Watanabe, Phys. Rev. B **2**, 2353 (1970).